

Measurement of the Carbon to Helium Ratio in Cosmic Rays from 2.1 GV to 1.8 TV with the Alpha Magnetic Spectrometer on the International Space Station

Melanie Heil*

On behalf of the AMS Collaboration

Massachusetts Institute of Technology, MIT, Cambridge, MA 02139, USA

E-mail: melanie.heil@cern.ch

The exact behavior of the carbon flux with rigidity and how it relates to the behavior of the helium flux is important for understanding charge dependencies of the production, acceleration and propagation mechanisms of charged cosmic rays in our galaxy. The current status of the measurement of the carbon flux and the carbon-to-helium ratio in primary cosmic rays with rigidities from 2.1 GV to 1.8 TV is presented based on data collected by the Alpha Magnetic Spectrometer in the first 40 month of operation on-board the International Space Station.

*The 34th International Cosmic Ray Conference,
30 July- 6 August, 2015
The Hague, The Netherlands*

*Speaker.

1. Introduction

Numerous measurements of the carbon flux in primary cosmic rays have been performed in the past by balloon and satellite experiments [1]. The exact behavior of the carbon flux with rigidity is important in understanding the production, acceleration and propagation mechanism of cosmic rays in our galaxy. The ratio of the carbon flux to the helium flux allows to test the charge dependence of these mechanisms. Here we report on the current status of a carbon flux analysis of data collected with the Alpha Magnetic Spectrometer (AMS) on the International Space Station (ISS) in its first 40 month of operation (May 2011 - Sep. 2014). Using our measurement of the helium flux with the same instrument [2], also the ratio of the carbon to helium flux is reported.

2. Detector

AMS is a general purpose high energy particle physics detector in space. The layout and description of the detector are presented in Ref. [3] and shown in Fig. 1.

The key elements used in this measurement are the permanent magnet, the silicon tracker, four planes of time of flight (TOF) scintillation counters, and the array of anticoincidence counters (ACC). AMS also contains a transition radiation detector (TRD), a ring imaging Čerenkov detector (RICH), and an electromagnetic calorimeter (ECAL). The AMS coordinate system is concentric with the magnet and above, below, and downward-going refer to the AMS coordinate system. Timing, location, and orientation are provided by GPS units affixed to AMS and to the ISS. The detector performance has been steady over time.

The tracker [4] has nine layers, the first (L1) at the top of the detector, the second (L2) just above the magnet, six (L3 to L8) within the bore of the magnet, and the last (L9) just above the ECAL. L2 to L8 constitute the inner tracker. The tracker accurately determines the trajectory of cosmic rays by multiple measurements of the coordinates. Together, the tracker and the magnet measure the rigidity (momentum/charge) $R = p/Z$ of charged cosmic rays.

Each layer of the tracker also provides an independent measurement of the absolute value of the charge $|Z|$ of the cosmic ray. Together, the charge resolution of the layers of the inner tracker is

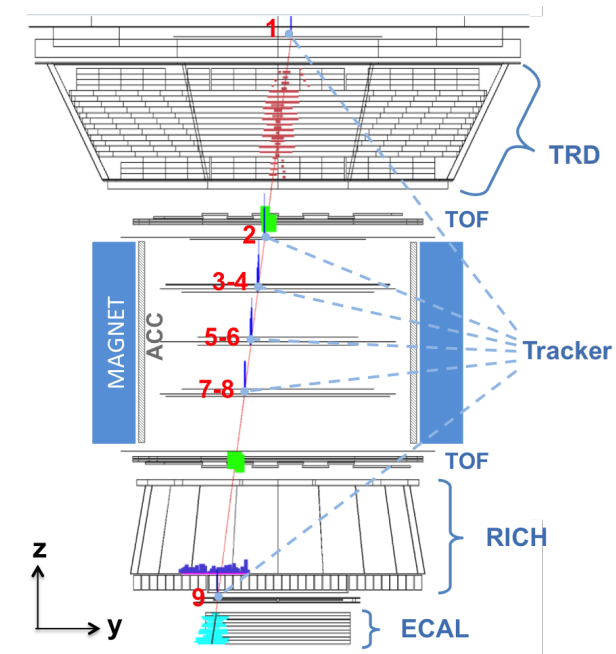


Figure 1: AMS-02 event display of a 169 GV carbon nuclei showing the detector profile in the y-z-plane.

$\Delta Z \simeq 0.12$ for $|Z| = 6$ particles.

Two planes of TOF counters [5] are located above L2 and two planes are located below the magnet. The overall velocity ($\beta = v/c$) resolution of the TOF discriminates between upward- and downward-going particles. The combination of the pulse heights of the two upper layers and the pulse heights of the two lower layers, respectively, provide independent measurements of the absolute charge, see Fig. 2.

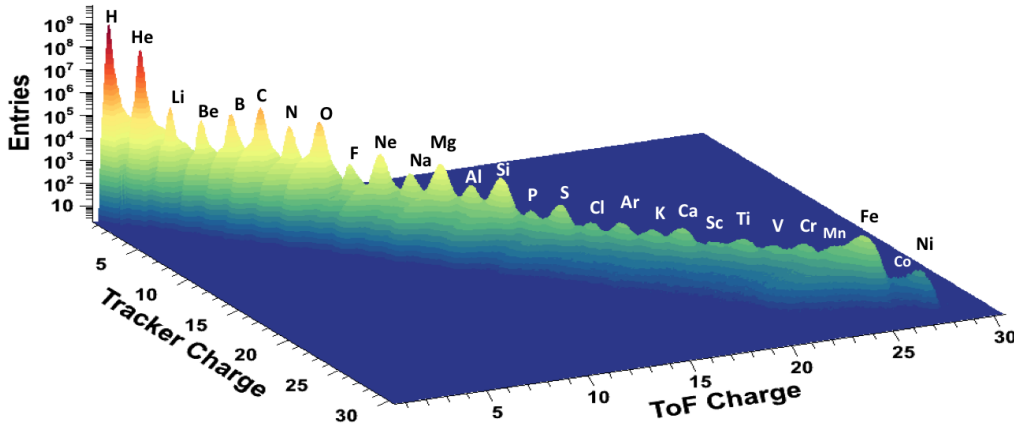


Figure 2: The charge measurement of primary cosmic rays with the inner tracker and the TOF. The multiple measurements of the charge along the particle trajectory allow for a clean nuclei selection and to identify interacting events.

The coincidence of signals from the four TOF planes together with signals from no more than four out of the eight read-out sectors of the ACC provides a charged particle trigger. The ACC has an efficiency of 0.99999 to reject cosmic rays with $|Z| = 1$ which enter the inner tracker from the side. The coincidence of 3 out of the 4 TOF layers without an ACC requirement was used to provide an unbiased trigger. Prescaled by 1/100, this was used to measure the efficiency of the charged particle trigger.

Monte Carlo (MC) simulated events were produced using a dedicated program developed by the collaboration based on the GEANT-4.10.1 package [6]. The program simulates electromagnetic and hadronic interactions of particles in the material of AMS and generates detector responses. The digitization of the signals is simulated precisely according to the measured characteristics of the electronics. The simulated events then undergo the same reconstruction as used for the data.

3. Selection

In the first 40 months AMS collected 5.3×10^{10} cosmic ray events. The collection time used in this analysis includes only those seconds during which the detector was in normal operating conditions, the AMS was pointing within 40° of the local zenith, the trigger live time exceeded 50%, and the ISS was outside of the South Atlantic Anomaly. Due to the influence of the geomagnetic field, this collection time for primary cosmic rays increases with increasing rigidity becoming constant at 8.5×10^7 s above 30 GV.

In order to have the best resolution at the highest rigidities, we require the track to pass through L1 and L9 and to satisfy additional track fitting quality criteria such as a $\chi^2/d.f. < 10$ in the bending coordinate. To remove the events which interacted within the detector, the charge as measured by each of L1, the upper TOF, the inner tracker, the lower TOF, and L9 is required to be compatible with $|Z| = 6$. To select only primary cosmic rays the measured rigidity is required to be greater than a factor of 1.2 times the maximum geomagnetic cutoff within the AMS field of view. The cutoff was calculated by backtracing [7] particles from the top of AMS out to 50 Earth's radii using the most recent IGRF [8] geomagnetic model. These procedures resulted in a sample of 1.4×10^6 primary cosmic rays with $Z = 6$.

Due to the multiple independent and accurate measurements of the absolute charge, the selected sample contains only a small contamination of particles with $Z \neq 6$ at tracker L1 of AMS. As shown in Fig. 3, the contamination with higher charge nuclei due to the charge resolution in tracker L1 was measured to be less than 0.2%. The sample also contains small amounts of carbon from other nuclei which interact at the top of AMS (for example, in L1). From the measured fluxes [9] and Monte Carlo simulation this contribution is estimated to be below 1% for the entire rigidity range. The background contributions are subtracted and their uncertainties are taken into account in the systematic error.

4. Analysis

The isotropic carbon flux Φ_i for the i^{th} rigidity bin $(R_i, R_i + \Delta R_i)$ is

$$\Phi_i = \frac{N_i}{A_i \varepsilon_i T_i \Delta R_i} \quad (4.1)$$

where N_i is the number of events corrected with the rigidity resolution function, A_i is the effective acceptance, ε_i is the trigger efficiency, and T_i is the collection time. In this analysis the carbon flux was measured in 66 bins, $i = 1$ to 66, from 2.1 GV to 1.8 TV with bin widths chosen according to the rigidity resolution. The acceptance A_i was calculated using the Monte Carlo simulation and then corrected for the small differences found between the data and the Monte Carlo event selection efficiencies. The trigger efficiency ε_i is measured to be greater than 99.5% for the whole rigidity range and the Monte Carlo simulation agrees with the measured trigger efficiency within 0.5%.

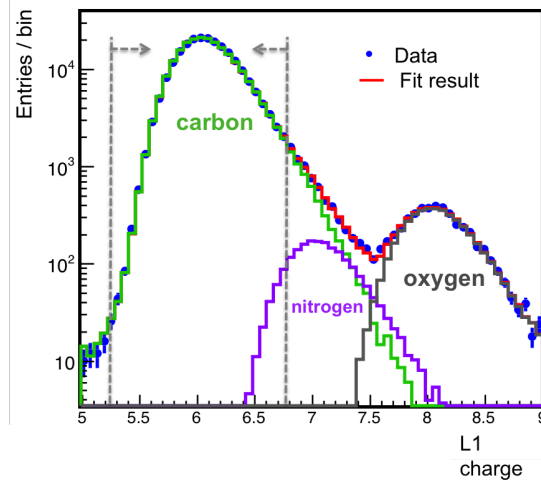


Figure 3: The charge distribution measured by tracker L1 for carbon selected by the inner tracker (L2-L8). The residual background from higher charge nuclei is determined by a template fit to the measured distribution and requiring that the measured charge is compatible with $|Z| = 6$ (gray lines).

The bin-to-bin migration of events was corrected using a rigidity resolution function, which was obtained from the simulated event samples and verified with the data. The correction for each bin was obtained using the iterative unfolding procedure described in Ref. [10].

Extensive studies were made of the systematic errors. These errors include the uncertainties in the trigger efficiency, the acceptance, the background contamination, the event selection, the unfolding, the rigidity resolution function, and the absolute rigidity scale. The trigger efficiency error is dominated by the statistics available from the 1% prescaled unbiased event sample. As the trigger efficiency is $> 99.5\%$, its corresponding systematic error is less than 0.5% over the whole rigidity range.

The acceptance was corrected for small differences between the data and the Monte Carlo samples related to the event reconstruction and selection. As an example, the ratio of the tracker L1 hit association efficiency to the inner tracker track between data and Monte Carlo simulation is shown in Fig. 4(a). The tracker L1 hit association verifies the simulation of elastic interactions of carbon with the detector, as small inefficiencies in this probability are due to scattering in the material of the TRD and the upper two TOF layers. As can be seen from Fig. 4(a), Data and Monte Carlo probabilities agree within 1%. The systematic error due to the effective acceptance estimation on the flux is less than 1.5% below 100 GV and reaches 4% at 1.8 TV.

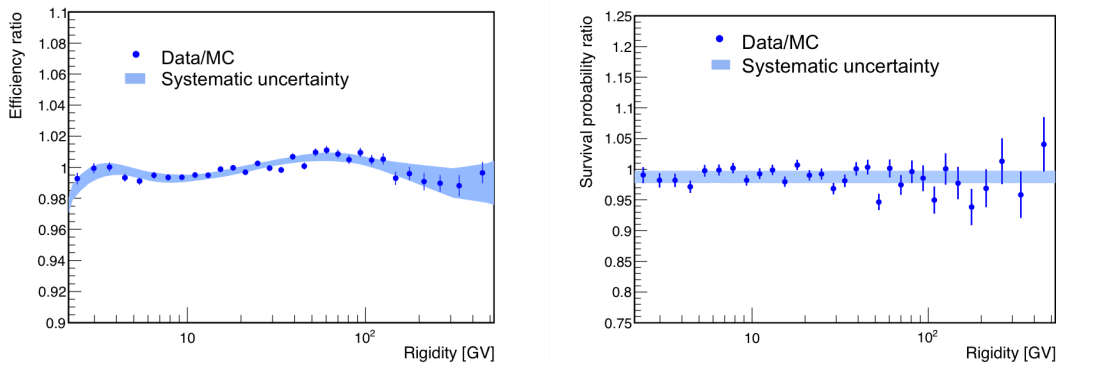


Figure 4: a) The ratio of the tracker L1 hit association efficiency to the inner tracker track between data and MC simulation together with its systematic uncertainty.

b) The ratio of the probability for carbon to interact between tracker L8 and L9, that is traversing the lower TOF and nearby materials, between data and MC simulation together with its systematic uncertainty.

The detector is mostly made of carbon and aluminum. The corresponding inelastic cross sections of C+C and C+Al have only been measured below 10 GV. The Glauber-Gribov model [6] of inelastic cross sections is used in the Monte Carlo calculation of the acceptance. To obtain the best agreement between the data and the simulation, dedicated samples were simulated with the inelastic cross sections scaled by $\pm 10\%$, $\pm 20\%$. Then the probability for carbon to interact between tracker L8 and L9, that is traversing the lower TOF and nearby materials, was calculated for data and for the simulated samples, for the best agreement see Fig. 4(b).

Using the obtained probabilities and the rigidity dependence of the cross sections from the model, the systematic error on the flux due to the uncertainty of Carbon inelastic cross sections

was evaluated to be 1.5% below 10 GV rising to 3% at 1.8 TV.

The rigidity resolution function for carbon was obtained from the Monte Carlo simulation and verified with the data. For this the difference between the coordinates measured in the individual tracker layers and those obtained from the track fit excluding the tested layer were compared between data and simulation, see Fig. 5.

Also, in order to validate the alignment of the external tracker layers the difference between the rigidities measured using the information from L1 to L8 and from L2 to L9 was compared between data and the simulation. The systematic errors due to the uncertainties of the rigidity resolution function were determined by varying the resolution function used in the unfolding procedure according to its uncertainties. Including the uncertainties from the unfolding procedure itself, they were found to be 1% below 200 GV and 3% at 1.8 TV.

There are two contributions to the systematic uncertainty on the rigidity scale, one from residual misalignment and the other from the magnetic field, discussed in detail in Ref. [10]. The corresponding error on the Carbon flux is below 0.6% up to 100 GV and reaches 4% at 1.8 TV.

Most importantly, several independent analyses were performed on the same data sample by different study groups. The current results of those analyses are consistent with the ones presented here.

5. Results

The measured carbon flux as a function of kinetic energy E_K with its total error, which is the quadratic sum of the statistical and the systematic errors, is shown in Fig. 6(a) together with the results of previous experiments [1]. For the conversion of the flux measured in rigidity to kinetic energy a pure sample of ^{12}C was assumed.

The current statistics of this measurement above 200 GV are not enough to distinguish between a single power law or double power law [2] behavior at high energies.

The flux ratio $\Phi(\text{C})/\Phi(\text{He})$ was calculated using the helium flux as measured by AMS [2]. As the interaction of carbon and helium with the detector are significantly different, only the error of the rigidity scale partially cancels in this measurement. The carbon to helium flux ratio as a function of rigidity is shown in Fig. 6(b). Below 45 GV the ratio is affected by solar modulation, as the carbon flux was measured in a longer time period as the helium flux and therefore was influenced by different solar activity. Above 45 GV the flux ratio is compatible with being constant, with large uncertainties at highest energies due to the low statistics in the carbon flux measurement.

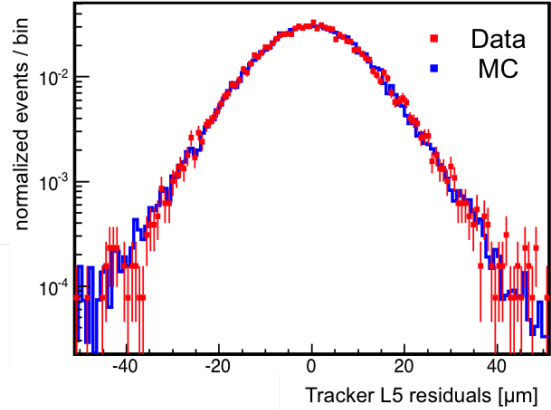


Figure 5: Difference between the coordinates measured in tracker L5 and those obtained from the track fit using tracker L2, L3, L4, L6, L7, L8 for both data (red) and MC simulation (blue).

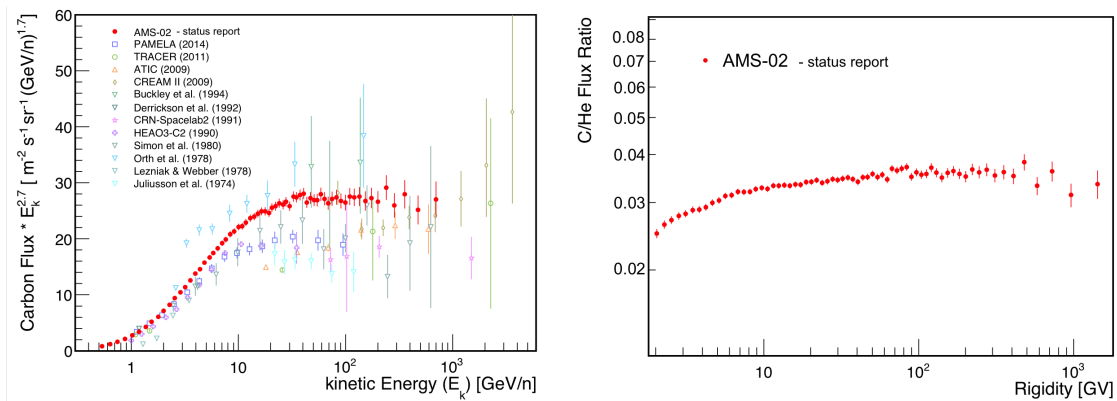


Figure 6: a) The flux as a function of kinetic energy per nucleon E_K multiplied by $E_K^{2.7}$ compared with recent measurements [1]. For the AMS results $E_K \equiv (\sqrt{12\bar{R}^2 + M^2} - M)/12$ where M is the ^{12}C mass. b) The AMS carbon to helium flux ratio as a function of rigidity.

In conclusion, knowledge of the carbon flux is important in understanding the origin, acceleration, and propagation of cosmic rays. Our measurement of the Carbon flux from 2.9 GV to 1.8 TV is currently based on 1.4 million events and detailed studies of the systematic errors. The carbon to helium flux ratio, which allows to test the charge dependence of the origin, acceleration, and propagation of cosmic rays, is compatible with being constant above 45 GV, with large uncertainties at highest energies due to the low statistics in the carbon flux measurement.

References

- [1] Panov *et al.*, *Bull. Russian Acad. Sci.* **73**, 564 (2009); Juliusson, *ApJ* **191**, 331 (1974); Orth *et al.*, *ApJ* **226**, 1147 (1978); Lezniak, Webber, *ApJ* **223**, 676 (1978); Derrickson *et al.*, *Int. J. Radiat. Appl. Instrum. D* **20**, 415 (1992); Simon *et al.*, *ApJ* **239**, 712 (1980); Buckley *et al.*, *ApJ* **429**, 736 (1994); Ahn *et al.*, *ApJ* **707**, 593 (2009); Muller *et al.*, *ApJ* **374**, 356 (1991); Engelmann *et al.*, *A&A* **233**, 96 (1990); Adriani *et al.*, *ApJ* **791**, 93 (2014); Obermeier *et al.*, *ApJ* **724**, 14 (2011);
- [2] The AMS Collaboration, *Precision Measurement of the Helium Flux in Primary Cosmic Rays from Rigidities of 1.9 GV to 3 TV with the Alpha Magnetic Spectrometer on the International Space Station*, (to be published).
- [3] A. Kounine, *Int. J. Mod. Phys. E* **21** 1230005 (2012); S. Rosier-Lees, in *Proceedings of Astroparticle Physics TEVPA/IDM*, Amsterdam, 2014 (to be published); S. C. C. Ting, *Nucl. Phys. B, Proc. Suppl.* **243-244**, 12 (2013); S.-C. Lee, in *Proceedings of the 20th International Conference on Supersymmetry and Unification of Fundamental Interactions (SUSY 2012)*, Beijing, 2012 (unpublished); M. Aguilar, in *Proceedings of the XL International Meeting on Fundamental Physics*, Centro de Ciencias de Benasque Pedro Pascual, 2012 (unpublished); S. Schael, in *Proceedings of the 10th Symposium on Sources and Detection of Dark Matter and Dark Energy in the Universe*, Los Angeles, 2012 (unpublished); B. Bertucci, *Proc. Sci. EPS-HEP*, **67** (2011); M. Incagli, *AIP Conf. Proc.* **1223**, 43 (2010); R. Battiston, *Nucl. Instrum. Methods Phys. Res., Sect. A* **588**, 227 (2008).
- [4] B. Alpat *et al.*, *Nucl. Instrum. Methods Phys. Res., Sect. A* **613**, 207 (2010).
- [5] V. Bindi *et al.*, *Nucl. Instrum. Methods Phys., Sect. A* **743**, 22 (2014) and references therein.

- [6] J. Allison *et al.*, *IEEE Trans. Nucl. Sci.* **53**, 270 (2006); S. Agostinelli *et al.*, *Nucl. Instrum. Methods Phys. Res., Sect. A* **506**, 250 (2003).
- [7] J. Alcaraz *et al.*, *Phys. Lett. B* **484**, 10 (2000);
- [8] C. C. Finlay *et al.* *Geophys. J. Int.* **183/3**, 1216 (2010). We have used data from IGRF-12 (2015), currently available at <http://www.ngdc.noaa.gov/IAGA/vmod/igrf.html> (unpublished).
- [9] The AMS Collaboration, *Measurement of the Flux of Light Nuclei in Primary Cosmic Rays with the Alpha Magnetic Spectrometer on the International Space Station*, (to be published).
- [10] M. Aguilar *et al.*, *Phys. Rev. Lett.* **114**, 171103(2015) ;
- [11] G. D. Lafferty, T.R. Wyatt, *Nucl. Instr. Methods Phys. Res., Sect. A* **355**, 541 (1995). We have used Eq. (6) with $\tilde{R} \equiv x_{lw}$.